# Photoluminiscent Manganese Nanoparticles from Solid State Polyphosphazenes Organometallic Derivatives

**Carlos Díaz[1,2] and María Luisa Valenzuela[1]**

Pyrolysis in air at 800°C of $[\{NP(OC_{12}H_{10})\}_{0.6}\{NP(OC_6H_4PPh_2\cdot(\pi\text{-}CH_3C_5H_4)-Mn(CO)_2)_2\}_{0.4}]_n$ (**1**) in the solid state affords product **2** containing nanoclusters of $Mn_2P_2O_7$ with sizes ranging from 50 to 90 nm and averaging about 74 nm. The egg-shape of the unpyrolyzed organometallic polymer is retained but with increased particle size after pyrolysis. The pyrolytic material shows near-infrared photoluminescence attributed to the emission of tetrahedral $Mn^{2+}$ embedded in a matrix of $Mn_2P_2O_7$. The solid-state pyrolysis of organometallic derivatives of polyphosphazenes may be a useful and general route to nano-structured $Mn_2P_2O_7$.

**KEY WORDS:** Manganese nanoparticles; Photoluminescent polymer; Polyphosphazene.

## 1. INTRODUCTION

Metal-containing nanoclusters (metal, metal oxide and other metal salts) are aggregates with as little as ten and as much as several thousand atoms in a single cluster [1, 2]. Typical cluster sizes are from approximately 10 to 100 nm. The properties of metal nanoclusters are interesting because they differ from those of the bulk material and individual atoms. Applications of these substances are being explored in the areas of advanced materials and heterogeneous catalysis [3, 4]. Metal nanoclusters can be prepared by a variety of techniques, including metal acid or salt reduction, metal evaporation, and sputtering. Almost all of these methods are carried out in the liquid phase, which may be in aqueous or nonaqueous organic solvents.

Stabilization of metal-containing nanoclusters is achieved by using alkane thiols [5], micelle surfactants [6], and polymers [7]. On the other hand, there are few techniques for the synthesis of metal-containing nanoclusters in the solid state [8–10].

Pyrolysis of poly(ferrocenylsilanes) in air yields a red crystalline material of composition $SiO_2/Fe_2O_3$ [8]. Solid state gold nanoparticles have been obtained by evaporating a toluene solution of Au nanoparticles, which have been generated in solution, and pyrolysis of the residue [9, 10]. Methods for preparing nano-structured metallic salts other than metals and metal oxides are very rare. To the best of our knowledge, there are no other examples in the literature of high temperature methods for producing nanostructured materials in the solid state, other than for metals and metal oxides, including nanostructured manganese species [1, 2]. Hence, pyrolysis of organometallic derivatives could be a useful method to obtain such materials. Unfortunately these routes have been virtually unexplored due to the lack of readily accessible, well-characterized transition metal-based macromolecules.

We previously reported the synthesis of a series of organometallic derivatives of polyphosphazenes [11–18]. In this paper we wish to report the solid state pyrolysis of the organometallic polyphosphazene, $[\{NP(OC_{12}H_{10})\}_{0.6}\{NP(OC_6H_4PPh_2\cdot(\pi\text{-}CH_3C_5H_4) Mn(CO)_2)_2\}_{0.4}]_n$ (**1**), the characterization of the pyrolytic product **2**, and the study of its photoluminescent properties.

[1] Department of Chemistry, Faculty of Sciences, University of Chile, Casilla, 653, Santiago, Chile.

[2] To whom correspondence should be addressed. E-mail: cdiaz @uchile.cl

## 2. EXPERIMENTAL

The synthesis of the mixed-polymer, $[\{NP(OC_{12}H_{11})\}_{0.6}\{NP(OC_6H_4PPh_2)_2\}_{0.4}]_n$ (**3**), was previously reported [14]. The pyrolysis experiments were performed by pouring weighed portions (0.05–0.15 g) of the organometallic polymer into aluminium oxide boats, which were placed in a tubular furnace under an air flow. A temperature program was used; i.e., heating from 25 to 300°C, annealing for 10 min, to 800°C, and annealing for 2 h. Yields of mixed polymer were in the range of 26–29%.

Thermogravimetric analysis (TGA) measurements were performed with a Mettler TA 4000. The polymer samples were heated at a rate of 10°C/min from ambient temperature to 1000°C under a constant flow of air.

IR spectra were recorded on an Perkin–Elmer 2000 FTIR Spectro-photometer. Raman spectra were obtained on a Dilor Instrument with a CCD detector. The light source was an $Ar^+$ laser emitting at 514 nm. Spectra were recorded in a 180° backscattering mode with 500-Mw laser powering. Measurements were made at room temperature on solid samples. An Olympus BX-40 microscope was attached to the Raman instrument. Photoluminescent spectra were recorded using the same Raman instrument.

Scanning electron microscope (SEM) images were made on a Philips EM 300 apparatus. Energy-dispersive X-ray analyses (EDAX) were performed using a Noran micro-probe that was attached to a JEOL 5410. Transmission electron microscope (TEM) images were made on a JEOL SX 100. The finely powdered samples were dispersed in water and dropped onto a conventional carbon-coated copper grid.

X-ray diffraction (XRD) was carried out at room temperature on a Siemens D-5000 diffractometer. The XRD data were collected using Cu–Kα radiation (40 KV and 30 mA).

## 3. RESULTS AND DISCUSSION

The mixed-polymer, $[\{NP(OC_{12}H_{11})\}_{0.6}\{NP-Cl_2\}_{0.4}]_n$ (**4**) was synthesized by the alkaline carbonate method [19, 20]. Incorporation of the organometallic fragment $(\pi\text{-}CH_3C_5H_4)Mn(CO)_2$ was achieved by reaction of the mixed-polymer (**3**) with the precursor, $HOC_6H_4PPh_2Mn(CO)_2(\pi\text{-}CH_3C_5H_4)$ (**4**), in tetrahydrofuran as a solvent [14]. Figure 1 is a schematic

formula of the organometallic polyphosphazene derivative.

As expected, pyrolysis in air produced a pale pink, almost colorless, solid. Characterization of this material by TEM (Fig. 2a) indicates the formation of metallic nanoclusters. A histogram of the material indicates some irregular shapes with nanoclusters from 50 to 100 nm, with most $\sim$74 nm (Fig. 2b). The EDAX analysis of the material (Fig. 2c) confirms the presence of manganese, oxygen, and phosphorus with a small amount of carbon. However, the percentages of these elements in several zones of the sample are somewhat different. The XRD powder patterns of the materials (Fig. 3) can be indexed to monoclinic $Mn_2P_2O_7$. In addition, the FTIR data indicate the presence of structures with P=O bonds, i.e. absorption at 1667, 733, 714 and 527 $cm^{-1}$ [21].

The morphology observed after calcination of the manganese–organometallic polymer was investigated by SEM. An irregular ovoid shape was found for the manganese polymer both before and after the pyrolysis, but with increased particle size after pyrolysis (Fig. 4).

Some insight into the mechanism of formation of $Mn_2P_2O_7$ from the organometallic polymer **1** can be obtained from the TGA in air (Fig. 5). The initial weight loss is attributed to the carbonization of the organic matter arising from the bispiro (clarify this) and $C_5H_4-CH_3$ and $OC_6H_4PPh_3$ groups (weight loss: found 63.82%, calculated 63.72%). The second weight loss corresponds to the formation of the volatile products $N_xO_Y$, $P_xO_Y$, and $H_2O$. The 33% pyrolytic residue (at 800°C) is close to that expected for $Mn_2P_2O_7$. The final 2.9% pyrolitic residue at
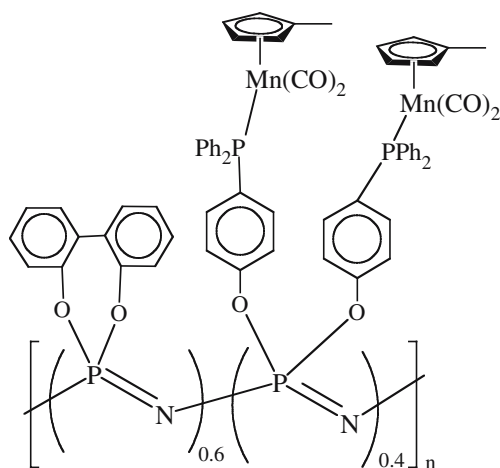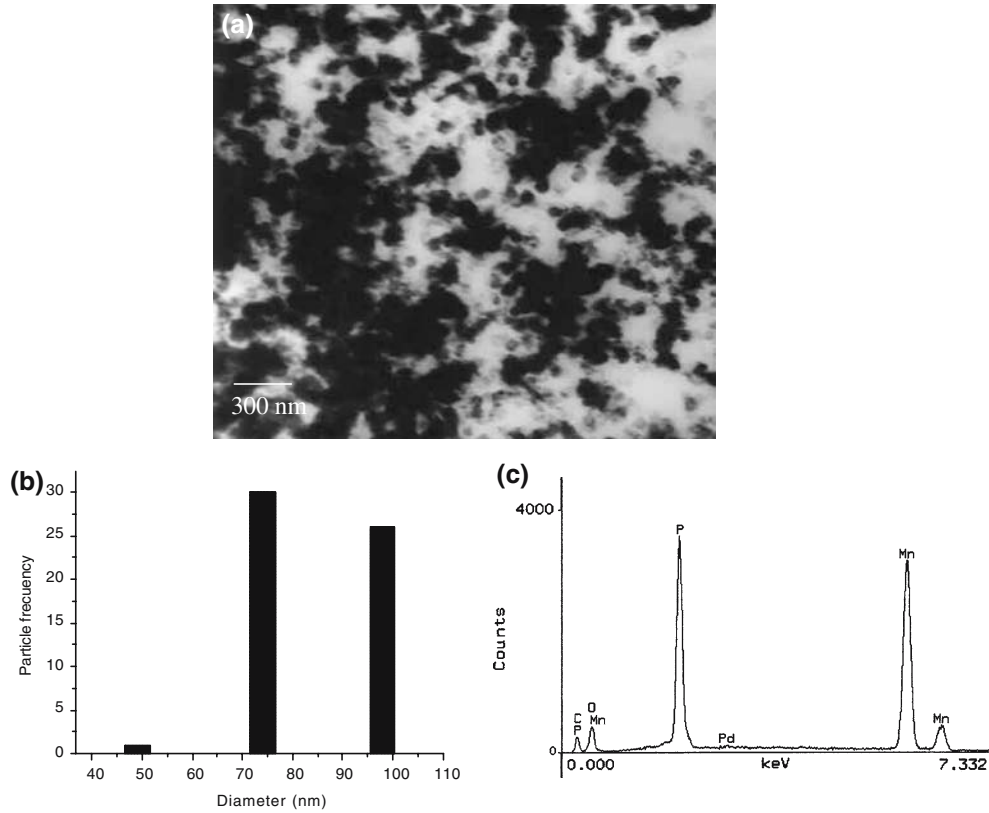


**Fig. 1.** Schematic structure of **1**.

**Fig. 2.** (a) TEM, (b) histogram, and (c) EDAX analysis of the pyrolytic residue **2**.

800°C indicates descomposition of the salt. It is at this point that the polyphosphazene acts as a hybrid organic–inorganic template in the solid state for formation of the metallic nanoparticles. The organic moiety, after calcinization, produces holes in the polymeric chains, which permit agglomeration of the metallic particles. The inorganic PN backbone of the polyphosphazenes in the presence of oxygen affords phosphorus atoms for the formation of the corresponding phosphate anions.
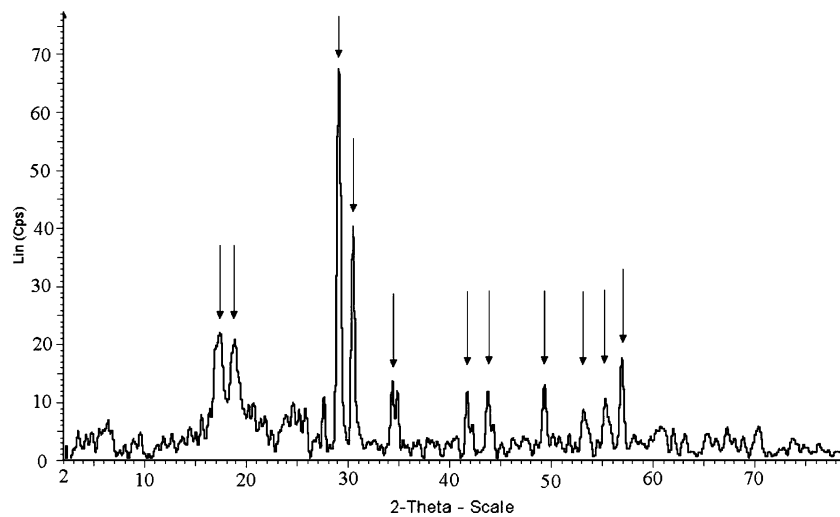


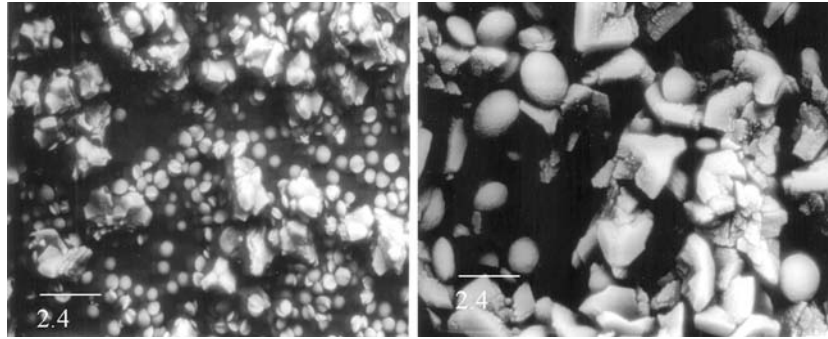**Fig. 3.** XRD pattern of **2**. The arrows indicate the peaks of monoclinic $Mn_2P_2O_7$.

**Fig. 4.** SEM image of the veterite disc of polymer **1**: (a) before calcination, and (b) after calcination.

The Raman spectrum of pyrolytic residue **2** shows luminescent behavior (Fig. 6a). The maximum of the photoluminescence spectrum is located at 1.93 eV (Fig. 6b).

This luminescence is similar to that obtained for $Mn^{2+}$ ions that are included in the matrixes of CdS [22–25], ZnS [26–28], ZnSe [29, 30], CdSe [31], $SnO_2$ [32], $CdCl_2$ [33], and InAs [34]. The luminescence is attributed to tetrahedrally coordinated $Mn^{2+}$ where

the emission arises from a $^4T_1(G) \rightarrow {}^6A_1(S)$ transition within the 3d shell of $Mn^{2+}$. For example, an emission band at 1.95 eV was reported for $Mn^{2+}$ ions in ZnSe [29]. The luminescence has been explained by Pileni [35]. According to this model, luminiscence for materials of the type $Mn_x$ and $M_yX_z$, where $M_yX_z$ is a semiconductor and the $x$ coefficient indicates a high $Mn^{2+}$ ion content, is caused by isolated tetrahedral $Mn^{2+}$ ions around a different $Mn^{2+}$ core (i.e. a
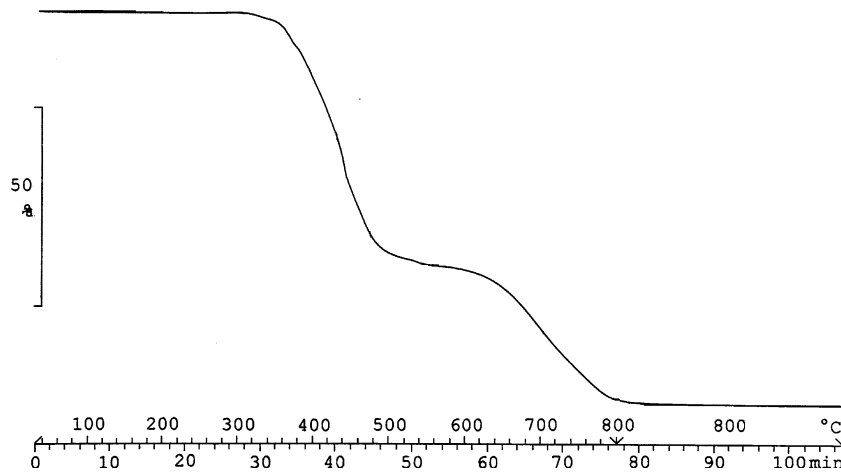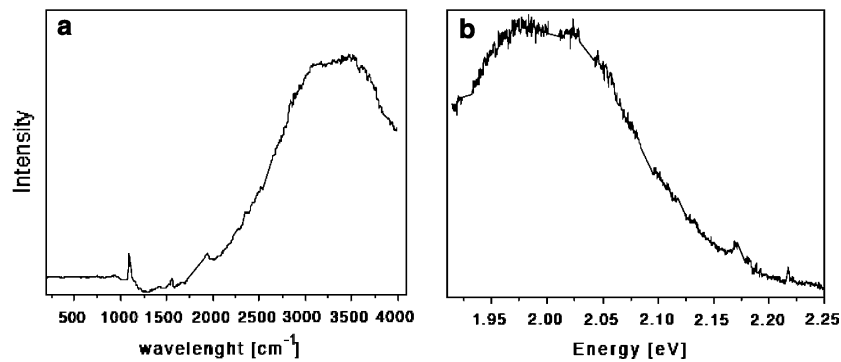


**Fig. 5.** TGA curve for **2**.



**Fig. 6.** (a) Raman spectrum of **2**. (b) Luminescence spectrum of **2**.

non-luminiscent octahedral $Mn^{2+}$). Thus the X-ray structure of $Mn_2P_2O_7$ indicates the presence of octahedral $MnO_6$ units [36]. This explanation of luminiscence is in agreement with observed variations in Mn content that was found by EDAX analysis. This case reported here represents the first example of luminiscence of isolated $Mn^{2+}$ ions that are embedded in a matrix containing non-luminiscent octahedral $Mn^{2+}$ ions as $Mn_2P_2O_7$. More significantly, the observed emission is similar to $Mn^{2+}$ nanoclusters that are embedded in some other $M_xP_yO_z$ salts, where M is Ca Zn, Sr, and Mg, but not Mn [37].

Inorganic luminescent solids have attracted attention due to their application in flat-panel color displays. It should be noted that the following commercial inorganic luminiscent phosphor-containing $Mn^{2+}$ have been developed: $Zn_2SiO_4{:}Mn^{2+}$, $MgF_2{:}Mn^{2+}$, $KMgF_3{:}Mn^{2+}$, $Zn_3(PO_4)_2{:}Mn^{2+}$, $MgSiO_3{:}Mn^{2+}$ [37]. Further work in this area in our laboratory is planned.

## 4. CONCLUSIONS

In this work we have described a new solid state synthesis of $Mn^{2+}$ embedded in $Mn_2P_2O_7$ nanoparticles. As far as we know, this is the first time that luminiscent $Mn^{2+}$ nanoparticles embedded in a non-luminiscent $Mn^{2+}$ matrix such as $Mn_2P_2O_7$ have been obtained by a solid state method. Since this method of synthesis makes it possible to obtain a solid state luminescent material based on nanostructured $Mn^{2+}$, it may be applied for the production of elecrooptical devices having possible uses in nanotechnology. On the other hand this is the first example were the polyphosphazene act as template in solid state in the formation of the metallic nanoparticles [38–41]. Other similar organometallic derivatives of polyphosphazenes have been reported by Allcock [42, 43], but their pyrolysis studies were not reported.

## ACKNOWLEDGMENTS

## REFERENCES

1. A. S. Edelstein and R. C. Cammarata, *Nanomaterials: Synthesis Properties and Applications* (J.W. Arrowsmith Ltda, Bristol, 2000).
2. K. J. Klabunde, *Nanoscale Materials in Chemistry* (Wiley-Interscience, New York, 2001).
3. J. Grunes, J. Zhu, G. A. Somorjai, *Chem. Comm.* 2257 (2003).
4. A. T. Bell, *Science* **299**, 1688 (2003).
5. J. C. Love, L. A. Estroff, J. K. Kriebel, R. G. Nuzzo, and G. M. Whitesides, *Chem. Rev.* **105**, 1103 (2005).
6. A. Roucoux, J. Schulz, and H. Patin, *Chem. Rev.* **102**, 3757 (2002).
7. C. Park, J. E. McAlvin, C. L. Fraser, and E. L. Thomas, *Chem. Mater.* **14**, 1225 (2002).
8. M. Ginzburg, M. J. MacLachlan, S. M. Yang, N. Coombs, T. W. Coyle, N. P. Raju, J. E. Greedan, R. H. Herber, G. A. Ozin, and I. Manners, *J. Am. Chem. Soc.* **124**, 2625 (2002).
9. T. Teranishi, S. Hasegawa, T. Shimizu, and M. Miyake, *Adv. Mater.* **13**, 1699 (2001).
10. T. Shimizu, T. Teranishi, S. Hasegawa, and M. Miyake, *J. Phys. Chem.* **107**, 2719 (2003).
11. C. Diaz and M. L. Valenzuela, in *Horizons in Polymers Research*, R. K. Bregg eds. (Nova Science Publishers, New York, 2005).
12. C. Díaz and P. Castillo, *J. Inorg. Organomet. Polym.* **11**, 183 (2001).
13. C. Díaz, P. Castillo, G. A. Carriedo, F. J. García Alonso, and P. Gómez-Elipe, *Macromol. Chem. Phys.* **203**, 1912 (2002).
14. G. A. Carriedo, F. J. García Alonso, P. A. González, C. Diaz, and N. Yutronic, *Polyhedron* **21**, 2579 (2002).
15. C. Díaz and P. Castillo, *Polym. Bull.* **50**, 12 (2003).
16. C. Díaz, M. L. Valenzuela, and M. Barbosa, *Mater. Res. Bull.* **39**, 9 (2004).
17. G. A. Carriedo, F. J. García Alonso, P. A. González, and P. Gómez-Elipe, *Polyhedron* **18**, 2853 (1999).
18. G. A. Carriedo, F. G. García-Alonso, J. L. García Álvarez, C. Díaz, and C. Yutronic, *Polyhedron* **21**, 2587 (2002).
19. G. Carriedo, L. Fernández-Catuxo, F. J. García-Alonso, P. Gómez-Elipe, and P. González, *Macromolecules* **29**, 5320 (1996).
20. G. Carriedo, F. García-Alonso, and P. González, *Macromol. Rapid Commun.* **18**, 371 (1997).
21. H. Seebert, *Anwendungen Der Schwing Bengsspektroskopie in Der Anorganishen Chemie* (Springer-Verlag, Berlin 1966) pp. 106, 107, 110.
22. G. Counio, T. Gacoin, and J. P. Boilot, *J. Phys. Chem. B.* **102**, 5257 (1998).
23. G. Counio, S. Esnouf, T. Gacoin, and J. P. Boilot, *J. Phys. Chem.* **100**, 20021 (1996).
24. L. Levy, N. Feltin, D. Ingert, and M. P. Pileni, *J. Phys. Chem. B.* **101**, 9153 (1997).
25. M. V. Artemyev, L. I. Gurinovich, A. P. Stupak, and S. V. Gaponenko, *Phys. Stat. Sol.* **224**, 191 (2001).
26. D. Denzler, M. Olschewski, and K. Sattler, *J. Appl. Phys.* **84**, 2841 (1998).
27. R. D. Yang, S. Tripathy, F. E. Tay, L. M. Gan, and S. J. Chua, *J. Vac. Sci. Tech. B.* **21**, 984 (2003).
28. K. Sooklal, B. S. Cullum, S. M. Angel, and C. J. Murphy, *J. Phys. Chem.* **100**, 4551 (1996).
29. J. Apperson, Y. Vorobiov, and G. F. J. Garlick, *Brit. J. Appl. Phys.* **18**, 389 (1967).
30. D. J. Norris, N. Yao, F. T. Charnock, and T. A. Kennedy, *Nanolett* **1**, 3 (2001).
31. F. V. Mikulec, M. Kuno, M. Bennati, D. A. Hall, R. G. Griffin, and M. G. Bawendi, *J. Am. Chem. Soc.* **122**, 2532 (2000).
32. F. Gus, F. Wang, M. K. Liu, G. Zhou, D. Xu, and D. Yuan, *J. Phys. Chem. B.* **108**, 8119 (2004).
33. V. Ghiordanescu, M. Sima, M. N. Grecu, and C. Ghice, *Roumanian. Rep. Phys.* **55**, 118 (2003).
34. C. A. Stowell, R. J. Wiacek, A. E. Saunder, and B. A. Korgel, *Nanolett* **3**, 1441 (2003).

35. L. Levy, N. Feltin, D. Ingert, and M. P. Pileni, *Langmuir* **15**, 3386 (1999).
36. T. Stefanidis and A. G. Nord, *Acta Cryst.* **C40**, 1995 (1984).
37. W. M. Yen and M. J. Weber, *Inorganic Phosphor: Compositions, Preparation and Optical Properties* (CRC Press, Boca Raton, New York, 2004).
38. Polyphosphazenes have been used as template for the formation of metal nanoparticles in solution: see refs. 39–41.
39. M. A. Olshavsky and H. R. Allcock, *Chem. Mater.* **9**, 1367 (1997).
40. C. H. Walker, St J. V. John, and P. Wisian-Neilson, *J. Am. Chem. Soc.* **123**, 3846 (2001).
41. J. Jung, T. Kmecko, C. L. Claypool, H. Zhang, and P. Wisian-Neilson, *Macromolecules* **38**, 2122 (2005).
42. H. R. Allcock, A. A. Dembeck, and E. H. Klingenberg, *Macromolecules* **24**, 5208 (1991).
43. H. R. Allcock, K. D. Lavin, N. M. Tollefson, and T. L. Evans, *Organometallics* **2**, 267 (1983).